Environmental Imaging with a Mobile UWB Security Robot for Indoor Localisation and Positioning Applications

Rahmi Salman, Ingolf Willms
Fachgebiet Nachrichtentechnische
Systeme (NTS)
Universität Duisburg-Essen
Duisburg, Germany
E-Mail: salman@nts.uni-due.de

Takuya Sakamoto, Toru Sato
Graduate School of Informatics
Kyoto University
Yoshida Honmachi, Sakyo-ku
Kyoto 606-8501, Japan

Alexander Yarovoy
Microwave Sensing, Signals and
Systems
Delft University of Technology
Delft, the Netherlands

Abstract—**In this paper environmental imaging of an unknown indoor area is performed by an autonomous mobile security robot called CoLORbot which operates with UWB-Radar. The CoLORbot is fully equipped with professional motion units, UWB-Radar devices, antennas and a laptop for data processing. Solitary objects are randomly distributed. The robot maintains a collision avoiding chaotic track and records UWB pulses throughout his inspection tour. Environmental imaging by means of UWB-Radar is performed with a migration algorithm as well as with the novel revised Range Point Migration method. These partial and fusioned maps of the environment allow an independent and self-localising capability of the CoLORbot and enable an autonomous navigation in an unknown environment.**

Keywords—Environmental imaging; Secuity robot; UWB Imaging; UWB Radar; revised RPM

I. INTRODUCTION

Hazardous scenarios full of dark dense smoke, dust and other particles as well as situations which are too dangerous for the security forces (e.g. at a nuclear disaster) ask for new generation sensing and Radar technologies. Depending on the circumstances, infrared, ultrasound, optics and narrowband Radar fail or at least are restricted immensely in performance. UWB technology has superior potential compared to these technologies. The microwave range is not only unaffected by particles in the air, it even establishes robustly through- and in-wall sensing due to the presence of low frequencies. Combined with high temporal and spatial resolution due to the huge bandwidth UWB-Radar provides multipath immunity to some extent. Furthermore, it enables coexistence with other narrowband radio systems due to its wideband combined with low power emission. M-sequence Radar devices become cost effective and small in dimensions which make them very attractive for the integration in mobile robot systems [1].

II. HARDWARE SETUP AND SYSTEM DESIGN

In this paper environmental imaging is performed with the CoLORbot in an indoor scenario with rich clutter distribution.

The ground plane of the investigated indoor scenario is depicted in Fig. 1.
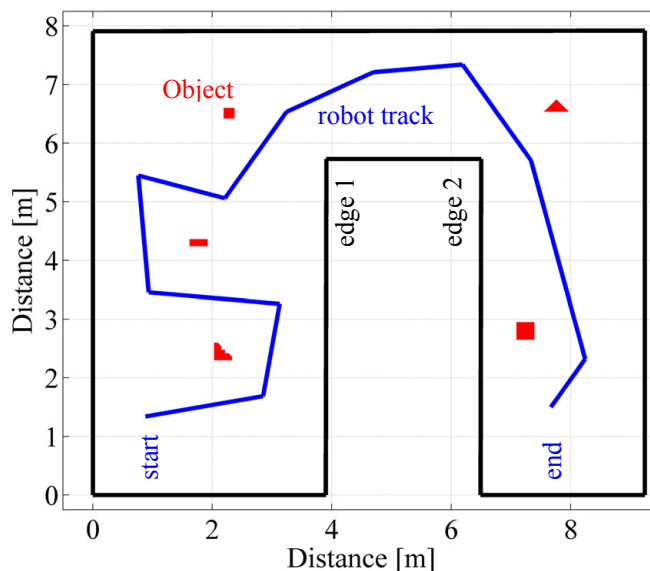
Figure 1. Schematic drawing of the measurement scenario.

To provide a realistic and not too simple indoor scenario with corners as well as edges and dimensions (56m^2) like that of a larger office room, the fire detection laboratory of the University Duisburg-Essen was modified and used as the location for the measurement campaign. To analyse the influence of the track, which finally generates the synthetic aperture, the first parts of the track (left block of the room) exhibit a different orientations making the track more chaotic by the rest (especially in the right block). Five solitary objects with cross sections up to 0.3 m were randomly distributed in the scenario.

A. The Mobile Security CoLORbot

An autonomous mobile security robot with professional motion units was fully equipped with UWB-devices, RF components, a power supply unit and a laptop for data acquisition and communication with the data fusion computer.

Schematic drawings of the robot as well as photographs are provided in Fig. 2.

angle servo
encoder motor
motor controller
UPS Inverter accumulator
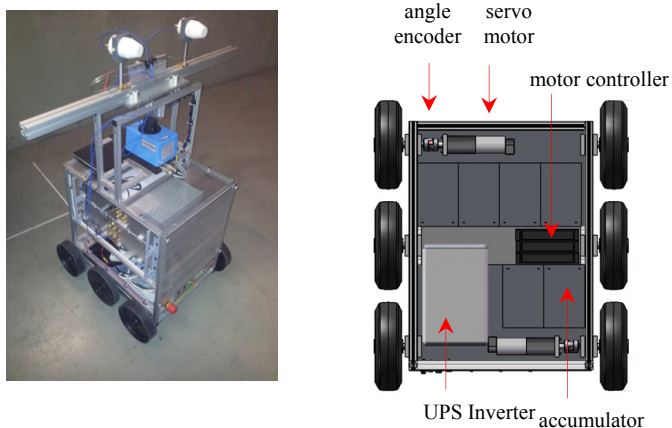
Figure 2. The mobile security robot CoLORbot with a schematic of the basement with crucial features.

The following description of the CoLORbot is taken from [1] where the authors have already addressed this issue previously: "If a mobile security robot is intended to assist these operations the design and equipment of the robot has to fulfil certain demands concerning motion accuracy. Therefore, some specifications have also been taken into account. There are totally three actuators in the robot, two in the motion unit at the bottom and one at the top which rotates the actual antenna array. The actuators are all hollow-shaft servo motors, which offer unique features unsurpassed by conventionally geared drives. Additionally, the gear ratio is set to 1:150 and is combined with a supplementary angle encoder with 500 Ticks per turn. This results in a sampling rate of 75000 samples per rotation for each actuator. The robot has 3 solid rubber tires at both sides which are connected by a chain-drive. To maintain a more gliding rotation of the robot with reduced errors the circumference of the middle tire is minimally higher than those of the other ones. The dimensions of the robot as well as the tire position maintain a rotation centre in the middle of the robot which also equals the middle of the antenna array at the top. Hence, the movement of the robot was entirely restricted to translations and rotations, strictly avoiding curvature paths. To further minimize erroneous robot motions the antenna array is equipped with its own rotational unit. The antenna alignment can be performed by just rotating the array, which is preferred compared to rotating the whole robot in case of an uneven floor."

B. Radar Device and Antennas

An UWB Maximum Length Binary Sequence (M-Sequence) Radar system with an operating band of DC–4.5 GHz was used within these investigations. For higher time resolution an additional quadrature modulator was used which operates with a carrier frequency of 9 GHz and doubles the bandwidth. Thus, the operating frequencies occupy the band of 4.5 GHz up to 13.5 GHz with an absolute bandwidth of 9 GHz and a fractional bandwidth of 100%. A pair of directive Teflon embedded two tapered slot line Vivaldi antennas on a single substrate [2][3] were mounted in bi-static configuration on the antenna array. The antennas have a satisfying matching with an s-parameter s11 less than 10dB in the whole range. With an antenna gain of up to 15 dBi and a narrow 3dB beam width of 25° the signal to noise ration is principally higher than e.g. isotropic antennas.

However, in many cases an immense effort for antenna alignment and regulating motions to properly gather spatially distributed energy in form of electromagnetic waves is needed. In worst case, the directive antennas will not recognize a nearby wall when they are improper aligned because the angle of reflection does not equal the angle of incidence with respect to the normal of the wall.

III. ENVIRONMENTAL IMAGING ALGORITHM

A. Challenges in Environmental Imaging

The inspection of randomly distributed solitary targets in the context of environmental imaging by means of electromagnetic waves in unknown indoor scenarios addresses following challenges:

- Due to the stationarity there is no speed difference between targets and the background.

- Unknown scenarios provide no background information which complicates the distinction of targets of interest and clutter.

- Indoor scenarios may result in dense clutter distribution. In worst case clutter occurs spatially close to targets of interest.

The concept of environmental imaging with a mobile security robot is based on synthetic aperture Radar (SAR). Instead of using one sensor with a large real aperture, the robot motion generates a synthetic aperture. Here, the CoLORbot was used with a speed of approximately 1 m/minute with a pulse repetition rate of 15 pulses/second. Within this inspection tour the environment interacts with the transmitted UWB pulses and is characterised by diffraction, reflection, and scattering. These effects are determined by the geometry of the objects, the operating frequency, the material composition and the polarisation of the incident wave. Within this paper the geometry of the environment shall be analysed and the remaining parameters are assumed to be constant or negligible. Thus, all received pulses have to be processed concerning their spatial and temporal signature subject to the local coordinate of the point of acquisition.

B. Imaging Algorithm - Revised Range Point Migration

A variety of imaging methods for UWB Radars have been developed [4][5][6][7][8][9]. Although one of the important features required by these security systems is fast calculation speed, many of the existing imaging methods do not satisfy this condition.. The revised range point migration (RRPM) has been proposed to quicken the computation for UWB radar imaging [10]. The RRPM is based on two principles: the inverse boundary scattering transform (IBST) [11] and weighted averaging to estimate stable derivatives of the target range in terms of the antenna position.

The IBST was originally derived for a mono-static radar, but can be also applied to bi-static radars under a certain condition. The IBST is expressed as

$$\begin{cases} x = X - Y \mathrm{d}Y/\mathrm{d}X \\ y = Y\sqrt{1-(\mathrm{d}Y/\mathrm{d}X)^2} \end{cases}, \quad (1)$$

where X is the x-coordinate of the antenna position and Y is the distance between the target and the antenna, which is estimated by extracting peaks of the received signals. Note that the coordinate system is translated and rotated so that the antenna scans on the x-axis. The derivative $\mathrm{d}Y/\mathrm{d}X$ is sensitive to noise and interference, making the IBST difficult to directly apply to complicated scenarios like in this paper. To stabilize the IBST, we developed the RRPM that estimates the derivative using weighted averaging of numerous peak points as

$$(\mathrm{d}Y/\mathrm{d}X)_i = \tan\left(\frac{\sum_{j \neq i} w_{i,j} \tan^{-1}\left(\frac{Y_i - Y_j}{X_i - X_j}\right)}{\sum_{j \neq i} w_{i,j}}\right), \quad (2)$$

$$w_{i,j} = \left|s_i s_j\right| \exp\left(-\frac{(X_i - X_j)^2}{\sigma_X^2} - \frac{(Y_i - Y_j)^2}{\sigma_Y^2}\right), \quad (3)$$

where X_i and Y_i are the i-th antenna position and the corresponding range, $w_{i,j}$ is the weighting coefficient that has a large value if $|Y_i - Y_j|$ and $|X_i - X_j|$ are both small. By averaging multiple points as in Eq. (2), the estimate of the derivative is statistically stabilized even for noisy data. We finally obtain the target image (x,y) by substituting Eq. (2) to Eq.(1). We set the parameters as $\sigma_X = 0.2$ m and $\sigma_Y = 0.2$ m in this paper.

C. Imaging Algorithm - Kirchhoff Migration

The second imaging algorithm used in this work is Kirchhoff migration (KM). KM is a basic imaging algorithm based on SAR principles which is extensively analysed in the literature [8]. Due to its low complexity and therewith simple adaption to given scenarios KM is widely used in the UWB-Radar community. The main idea is a back projection of the radiation characteristic and relies on some form of coherent summation. This means that a pixel of the Radar image is produced by integrating the phase-shifted Radar data of each antenna position. N measurements contribute to the value of a pixel with (x,y)-coordinate which can be mathematically formulated as

$$p(x,y) = \frac{1}{N}\sum_{n=1}^{N} h_n\left(\frac{d_{TXn} + d_{RXn}}{c_0}\right). \quad (4)$$

Here, $h_n(t)$ is the n-th measured impulse response in time domain, d_{TXn} and d_{RXn} are the distances between $p(x,y)$ and the transmit and receive antenna, respectively. The speed of light is c_0. In case of a bi-static configuration this algorithm summarises the impulse response values along ellipses. At positions where objects cause a reflection and therewith

increase the values in the impulse response, the ellipses superpose to image spots of high intensity. The image contrast is higher with increasing number of recorded impulse responses at different positions.

However, the superposition also leads to image artefacts because the ellipses do not only intersect at object locations. Hence, this ambiguity of intersection of ellipses decreases the spatial resolution and causes erroneous hot spots. Moreover, even in an image area where the ellipses do not intersect the noise floor is increased by the ellipses themselves which reduces the signal to noise and signal to clutter ratio. To some extent and under special circumstances (dense clutter with positions near to objects of interest) these artefacts can make the interpretation of the resulting image difficult or even impossible.

IV. EXPERIMENTALLY VALIDATED RESULTS

The antennas are throughout the investigation used in bi-static configuration positioned on the array with a distance of 0.15 m to the rotation axis. Every 20 cm of the track the robot stops and the array performs a full rotation while gradually making measurements. For KM a dynamic meshgrid of 6m x 6m was used around each rotation centre. The resulting sub-images were merged together for the final image of the whole scenario which is presented in Fig. 3.

The influence of noise is very low resulting in a high dynamic range. Due to the more chaotic track at the beginning of the track the imaging is more robust resulting in object surfaces which are nearly recognisable. At the end of the track this effect is weaker because of the linear aperture and the objects are sensed on a drive-by track rather on a circular track. This is to some extent quite plausible and is not a criterion for error-proneness. In Fig. 4 the same image is shown in a topology version with altitude information. Actually, a low number of artefacts or phantom hot spots can be seen
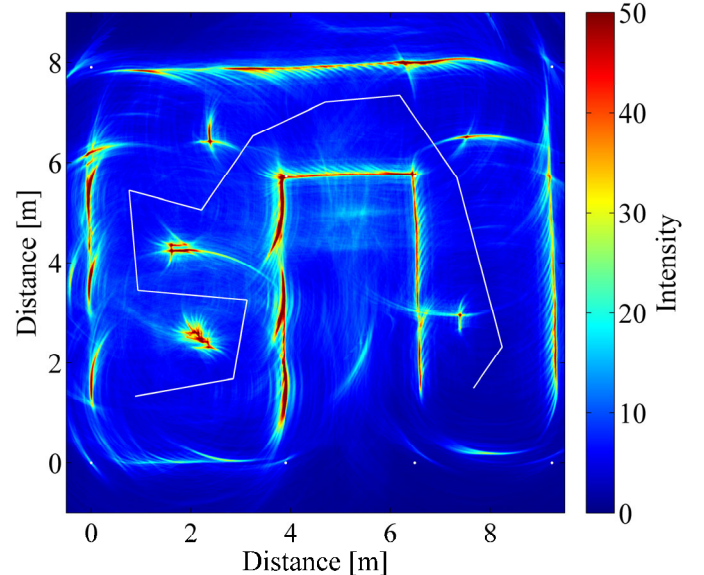
Figure 3. Full image obtained with the KM.

Figure 4. 3D altitude image obtained with the KM.

Fig. 5 shows the image obtained using the RRPM. Although the original image obtained using Eq. (1) is expressed as a cluster of points, each point is projected to the grid data with a weight of the signal amplitude. The image clearly shows the room walls and five targets, whereas the artefacts are suppressed thanks to the averaging process in Eq. (2).
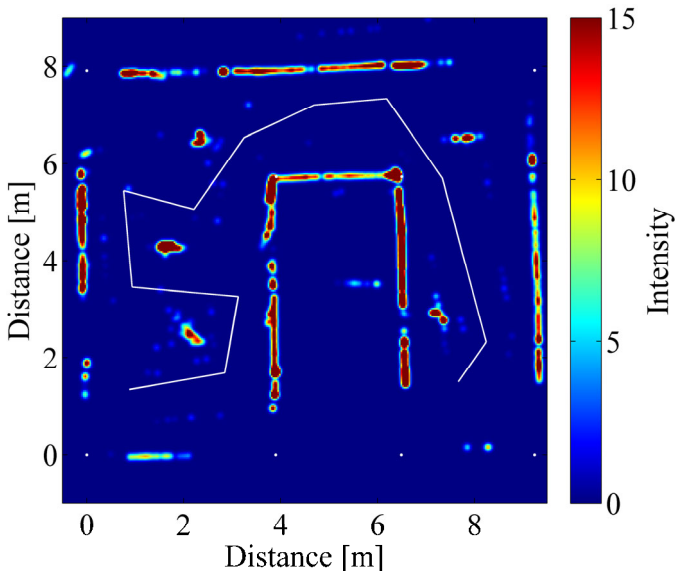
Figure 5. Image obtained with the RRPM.

Both images provide a characterisation of the environment in a way which allows to some degree the robot to inspect the room and complete its track avoiding collisions. Due to the vast computational load of the KM this can be solved real-time only with the RRPM.

V. CONCLUSION

Environmental imaging by means of UWB technology performed by an autonomous security robot in an unknown indoor scenario is a resolvable challenge. Both imaging algorithms (KM and RRPM) provide a map in an adequate quality. However, the novel RRPM provides a very fast calculation and is real-time capable which makes it very attractive for security operations. Measurement results demonstrate the extraction of features like the structure of the room or solitary objects in sufficient quality for positioning purposes. It is a more promising strategy to use the track as chaotic as possible, because this creates a more non-linear synthetic aperture. This map allows an independent and self-localising capability relative to the surrounding of a security robot and enables an autonomous navigation in an unknown environment.

REFERENCES

[1] R. Salman, I. Willms, "A Mobile Security Robot equipped with UWB-Radar for Super-Resolution Indoor Positioning and Localisation Applications", 2012 IEEE International Conference on Indoor Positioning and Indoor Navigation (IPIN), Sydney, Australia, Nov. 2012.

[2] R. Zetik, H. Yan, E. Malz, S. Jovanoska, G. Shen, R.S. Thomä, R. Salman, T. Schultze, R. Tobera, I. Willms, L. Reichardt, M. Janson, T. Zwick, W.Wiesbeck, T. Deißler, J. Thielecke. "*Cooperative Localization and Object Recognition*" in UKoLoS Ultra-Wideband Radio Technologies for Communications, Localization and Sensor Applications. R.S. Thomä, R. Knöchel, J. Sachs, I. Willms, T. Zwick (Eds.). InTech Academic Publisher, ISBN: 978-953-51-0936-5.

[3] R. Salman, I. Willms, L. Reichardt, T. Zwick, W. Wiesbeck, "On Polarization Diversity Gain in Short Range UWB-Radar Object Imaging", 2012 IEEE International Conference on Ultra-Wideband (ICUWB), Syracuse, USA, Sept. 2012.

[4] D.L. Mensa, D. Heidbreder, G. Wade, "Aperture synthesis by object rotation in coherent imaging," IEEE Trans. Nucl. Sci., vol. NS-27, no. 2, pp. 989-998, Apr. 1980.

[5] D. Liu, J. Krolik, L. Carin, "Electromagnetic target detection in uncertain media: Time-reversal and minimum-variance algorithms," IEEE Trans. Geosci. Remote Sens., vol. 45, no.4, pp. 934-944, Apr. 2007.

[6] R. H. Stolr, "Migration by fourier transform," Geophysics, vol. 43, no. 1, pp. 23-48, Feb. 1978.

[7] A. G. Yarovoy, T. G. Savelyev, P. J. Aubry, P. E. Lys, L. P. Ligthart,"UWB array-based sensor for near-field imaging," IEEE Transactions on Microwave Theory and Techniques, vol. 55, no. 6, part 2, pp. 1288-1295, June 2007.

[8] X. Zhuge, A. G. Yarovoy, T. Savelyev, L. Ligthart, "Modified Kirchhoff migration for UWB MIMO array-based radar imaging" IEEE Transactions on Geoscience and Remote Sensing, vol. 48, no. 6, pp. 2692–2703, 2010.

[9] X. Zhuge, and A. Yarovoy, "A sparse aperture MIMO-SAR based UWB imaging system for concealed weapon detection," IEEE Transactions on Geoscience and Remote Sensing, vol. 49 no. 1, pp. 509–518, 2011.

[10] T. Sakamoto, T. Savelyev, P. Aubry, A. Yarovoy, "Fast Range Point Migration Method for Weapon Detection using Ultra-Wideband Radar," IEEE 9th European Radar Conference, EuRAD, 31.10.-02.11.2012, Amsterdam, The Netherlands.

[11] T. Sakamoto, T. Sato, "A target shape estimation algorithm for pulse radar systems based on boundary scattering transform," *IEICE Trans. Commun.* vol. E87-B, No.5, pp.1357-1365, May, 2004.